UNIVERSITY OF AMSTERDAM

UvA-DARE (Digital Academic Repository)

Size-exclusion chromatography using core-shell particles

Pirok, B.W.J.; Breuer, P.; Hoppe, S.J.M.; Chitty, M.; Welch, E.; Farkas, T.; van der Wal, S.; Peters, R.; Schoenmakers, P.J.

DOI
10.1016/j.chroma.2016.12.015

Publication date
2017

Document Version
Final published version

Published in
Journal of Chromatography A

License
Article 25fa Dutch Copyright Act (https://www.openaccess.nl/en/in-the-netherlands/you-share-we-take-care)

Link to publication

Citation for published version (APA):
Pirok, B. W. J., Breuer, P., Hoppe, S. J. M., Chitty, M., Welch, E., Farkas, T., van der Wal, S., Peters, R., & Schoenmakers, P. J. (2017). Size-exclusion chromatography using core-shell particles. *Journal of Chromatography A*, *1486*, 96-102. https://doi.org/10.1016/j.chroma.2016.12.015

General rights
It is not permitted to download or to forward/distribute the text or part of it without the consent of the author(s) and/or copyright holder(s), other than for strictly personal, individual use, unless the work is under an open content license (like Creative Commons).

Disclaimer/Complaints regulations
If you believe that digital publication of certain material infringes any of your rights or (privacy) interests, please let the Library know, stating your reasons. In case of a legitimate complaint, the Library will make the material inaccessible and/or remove it from the website. Please Ask the Library: https://uba.uva.nl/en/contact, or a letter to: Library of the University of Amsterdam, Secretariat, Singel 425, 1012 WP Amsterdam, The Netherlands. You will be contacted as soon as possible.

UvA-DARE is a service provided by the library of the University of Amsterdam (https://dare.uva.nl)

Download date:09 Aug 2024

Journal of Chromatography A, 1486 (2017) 96–102

Contents lists available at ScienceDirect

Journal of Chromatography A

journal homepage: www.elsevier.com/locate/chroma

Size-exclusion chromatography using core-shell particles

Bob W.J. Pirok[a,b,*], Pascal Breuer[a], Serafine J.M. Hoppe[a], Mike Chitty[c], Emmet Welch[c], Tivadar Farkas[c], Sjoerd van der Wal[a], Ron Peters[a,d], Peter J. Schoenmakers[a]

[a] University of Amsterdam, van't Hoff Institute for Molecular Sciences, Analytical-Chemistry Group, Science Park 904, 1098 XH Amsterdam, The Netherlands
[b] TI-COAST, Science Park 904, 1098 XH Amsterdam, The Netherlands
[c] Phenomenex Inc., 411 Madrid Ave., Torrance, CA 90501, USA
[d] DSM Coating Resins, Sluisweg 12, 5145 PE Waalwijk, The Netherlands

ARTICLE INFO

Article history:
Received 13 September 2016
Received in revised form 5 December 2016
Accepted 8 December 2016
Available online 14 December 2016

Keywords:
Core-shell particles
Size-exclusion chromatography
Sec
Uhplc
Specific resolution
Packing resolution factor

ABSTRACT

Size-exclusion chromatography (SEC) is an indispensable technique for the separation of high-molecular-weight analytes and for determining molar-mass distributions. The potential application of SEC as second-dimension separation in comprehensive two-dimensional liquid chromatography demands very short analysis times. Liquid chromatography benefits from the advent of highly efficient core-shell packing materials, but because of the reduced total pore volume these materials have so far not been explored in SEC.

The feasibility of using core-shell particles in SEC has been investigated and contemporary core-shell materials were compared with conventional packing materials for SEC. Columns packed with very small core-shell particles showed excellent resolution in specific molar-mass ranges, depending on the pore size. The analysis times were about an order of magnitude shorter than what could be achieved using conventional SEC columns.

© 2016 Elsevier B.V. All rights reserved.

1. Introduction

Synthetic polymers are of indisputable value in modern day society. One critical factor in studying polymers and polymerization processes is the molar-mass distribution (MMD; or, equivalently, the molecular-weight distribution, MWD), which is generally determined by size-exclusion chromatography (SEC). Separation in SEC is achieved through partial exclusion of molecules from the pores of the stationary phase [1]. Molecules that are too large to enter the pores (*i.e.* are excluded) will travel through the column faster than molecules which do permeate into the pores. Smaller molecules will penetrate a larger volume of the pores, hence reside longer in the column and elute later. Consequently, sample-solvent molecules are observed as the latest eluting peak in SEC. It is essential that the mobile phase is a strong enough solvent to avoid any (enthalpic) interaction between the analyte polymers and the solid surface of the packing material, which would jeopardize the size-based separation and might cause analytes to elute later, in some cases after the solvent band. A polydisperse homopolymer will elute from the SEC column as a broad band (corresponding to a broad molecular size distribution). Other, more complicated (multimodal) distributions may be encountered for heterogeneous polymers, polymer blends, etc. After recording a calibration curve using narrowly distributed reference standards, the broad distribution can be translated into the MMD.

Fast SEC is of interest in high-throughput applications, such as in combinatorial-chemistry studies, where up to one hundred samples may be generated within a single day [2]. However, analysing a hundred samples per day (including standards) would necessitate SEC analysis times within, say, ten minutes. Very fast SEC is of specific interest as second dimension separation in comprehensive two-dimensional (2D) liquid chromatography (LC × LC) [3,4]. In LC × LC, all effluent from a first-dimension column is transferred to, and separated by, a second-dimension column. In such 2D separation systems, an additional separation dimension (*e.g.* reversed-phase liquid chromatography) can provide complementary information. For example, the chemical composition distribution (CCD) and the MMD can be monitored simultaneously. In order to maintain the first-dimension separation, it should be sampled sufficiently often. This induces the requirement of the second-dimension method to be fast, so as to complete the elution of one fraction before the next fraction from the first-dimension is transferred and injected. The key objective for the

* Corresponding author at: University of Amsterdam, van't Hoff Institute for Molecular Sciences, Analytical-Chemistry Group, Science Park 904, 1098 XH. Amsterdam, The Netherlands.
E-mail address: B.W.J.Pirok@uva.nl (B.W.J. Pirok).

http://dx.doi.org/10.1016/j.chroma.2016.12.015
0021-9673/© 2016 Elsevier B.V. All rights reserved.

second-dimension separation in LC × LC is to obtain the best possible resolution in the shortest possible time [5,6].

Because SEC is the method of choice for MMD determination, the technique is applied routinely in laboratories of polymer manufacturers and a great deal of work has been carried out to increase the speed of analyses [7]. The advent of pressure-resistant fully porous sub-2-μm stationary-phase particles, has allowed the efficiencies of polymer separations in SEC to be further optimized to create ultra-high pressure SEC (UHPSEC) [8]. Using UHPSEC, Janco et al. achieved a reduction in analysis time for the separation of polymer standards by approximately a factor of ten relative to conventional SEC [9]. Uliyanchenko et al. used UHPSEC as second dimension in an LC × LC separation system combined with (ultra-high pressure) RPLC in the first dimension for the separation of PMMA and PBMA homo- and copolymers, and polyurethanes [4].

The usefulness of SEC is mainly determined by the column performance or resolution of the used method. This is true for all SEC separations, but it can be most clearly illustrated when multimodal distributions or mixtures of polymers are to be characterized. In chromatography, resolution is given by

$$R_s = \frac{\Delta V_e}{2(\sigma_1 + \sigma_2)} \approx \frac{\Delta V_e}{4\sigma} \quad (1)$$

where V_e is the elution volume of the peak and sigma is a measure of the analyte bandwidth in volume units. This classical definition is, however, not very useful in SEC, where resolving individual species is not the aim of the analysis. Instead, we are generally interested in the ability of the SEC column to distinguish between molecules of the same polymer differing in molar mass. For two such polymers with (average) molar masses M_1 and M_2 the SEC resolution can be described within an (approximately) linear section of the SEC calibration curve with slope b [1,10]

$$\Delta V_e = \left(V_{e,2} - V_{e,1}\right) = \frac{\log(M_1/M_2)}{b} \quad (2)$$

where the subscript 1 denotes the first eluting peak and 2 the second eluting peak. Thus, $\Delta V_e > 0, M_1 > M_2$ and $b > 0$.

Substitution of Eq. (2) into Eq. (1) yields

$$R_s = \frac{\log(M_1/M_2)}{2b(\sigma_1 + \sigma_2)} \cong \frac{\log(M_1/M_2)}{4\sigma \cdot b} \quad (3)$$

The last part of Eq. (3) is valid in the molar mass range where the performance of the SEC column is independent of the molar mass of the polymer analytes. This simplification suffices for the present discussion. A useful figure of merit is obtained by assuming that the two analyte polymers differ in molar mass by one order of magnitude ($M_1/M_2 = 10$), in which case we obtain the specific resolution $\left(R_{sp}\right)$,

$$R_{sp} = \frac{0.25}{\sigma \cdot b} \quad (4)$$

Eq. (4) is especially useful for the comparison of different SEC systems (columns, instrument and separation conditions), irrespective of the molar masses of the analytes (within the linear range with negative slope b).

This concept can be further adapted to allow the comparison of different column packings by normalizing for the column length L to obtain the normalized specific resolution, or packing resolution factor [1], which is defined as

$$R^*_{sp} = \frac{0.25}{\sigma \cdot b\sqrt{L}} \quad (5)$$

It is important to note that, unlike the classical resolution R_s (Eq. (1)) and the specific (SEC) resolution R_{sp} (Eq. (4)), which are both dimensionless, R^*_{sp} has a dimension of length units to the power of − ½ (*e.g.* $mm^{-½}$).

An exciting development to enhance the performance of LC has been the (re-) introduction of core-shell particles. Excellent chromatographic efficiency has been achieved by using this types of packing materials [11,12]. However, this development has been ignored by the field of SEC, because the largest possible pore volume is thought to be an optimal factor for SEC [1]. While it is true that the presence of a solid core inside the particle implies a lower pore volume of the particle as a whole, this does not necessarily mean that efficient SEC using core-shell particles is not feasible. For example, in the event of a typical particle with a diameter of 2.6 μm with a solid core of 1.9 μm, the volume of the solid core is approximately 3.6 pL, whereas the total volume of the entire particle is about 9.2 pL. Indeed, the reduction in pore volume for a core-shell 2.6 μm particle relative to a fully porous particle of identical size is about 40%. We find it worthwhile to explore whether good SEC separations can be achieved using highly efficient core-shell particles, despite this somewhat reduced pore volume. The results of this feasibility study are presented in this paper.

2. Experimental

2.1. Instrumental

All experiments were carried out on an Agilent 1290 Infinity 2D-LC (Agilent Technologies, Waldbronn, Germany) system configured for one-dimensional operation. The used chromatographic setup comprised a binary pump (G4220A), a diode-array detector (G4212A) equipped with an Agilent Max-Light cartridge cell (G4212-6008, 10 mm, V_{det} = 1.0 μL), an autosampler (G4226A) and a thermostatted column compartment (G1316C). In front of the column, an Agilent 1290 Infinity in-line filter (G5067-4638) was installed for protection. The extra-column volume was approximately 36 μL. The injector needle was set to draw and eject at a speed of 10 μL/min with 2 s equilibration time. The entire system was controlled using Agilent OpenLAB CDS Chemstation Edition (Rev. C.01.04) software. The investigated columns are listed in Table 1.

2.2. Chemicals

Sudan IV (catalogue #: 198102-25G, CAS #: 85-83-6) and toluene (99.9%, CHROMASOLV® HPLC grade, catalogue #: 34886, CAS#: 108-88-3) were obtained from Sigma-Aldrich (Darmstadt, Germany). Acetonitrile (ACN, LC–MS grade) and non-stabilized tetrahydrofuran (THF, HPLC-S grade) were obtained from Biosolve (Valkenswaard, The Netherlands). Polystyrene standards (PS) for determining calibration curves were obtained from Polymer Laboratories (now Agilent Technologies, Church Stretton, Shropshire, UK). The specified peak molar masses and molar mass dispersities of all PS standards are displayed in Table 2. All PS standards were dissolved in THF in concentrations of approximately 0.2 mg mL^{-1}. To ensure the absence of molecular crowding or viscous-fingering effects at this concentration, concentration series were recorded for several polymers of a high molar mass. No effects of the concentration on the peak shape or position were observed (See Supplementary Data Figs. S2 and S3).

2.3. Analytical methods

For measuring calibration curves, toluene and each of the PS-standard solutions were injected separately onto each column with blank injections after every five analyte injections. Each calibration curve was measured at least three times, the precision was found to be good (RSD < 0.3% at n = 5. See Supplementary Material Tables S1 and S2, and Fig. S1 for additional data concerning the precision.). The mobile phase used was non-stabilized THF. The detection

Table 1
Overview of investigated columns.

ID	Manufacturer	Dimensions[a] (mm)	Particle size (μm)	Pore size (Å)	Particle type	Material	Pressure (bar)	Flow rate (mL/min)	Corr. coefficient[c]
1	Phenomenex	100 × 2.1	1.3	86	core-shell	silica	1030[e]	0.65	0.9746
2	Phenomenex	150 × 4.6	3.6	175	core-shell	silica (C18)	585	4[d]	0.9705
3	Phenomenex	150 × 4.6	2.6	98	core-shell	silica	850	4[d]	0.9663
4	Phenomenex	150 × 4.6	2.9	172	core-shell	silica	880[e]	3	0.9575
5	Phenomenex	150 × 4.6	3.6	477	core-shell	silica	436	4[d]	0.9937
6	Phenomenex	150 × 4.6	3.6	328	core-shell	silica	466	4[d]	0.9951
7	Phenomenex	150 × 4.6	3.6	199	core-shell	silica	463	4[d]	0.9961
8	Phenomenex	150 × 4.6	2.6	98	core-shell	silica (C18)	762	4[d]	0.9969
9	Phenomenex	150 × 4.6	3.6	477	core-shell	silica (C18)	563	4[F]	0.9911
10	Phenomenex	150 × 4.6	3.6	328	core-shell	silica (C18)	562	4[d]	0.9812
11	Phenomenex	150 × 4.6	3.6	190	core-shell	silica (C18)	788	4[d]	0.9759
12	Phenomenex	100 × 2.1	1.3	88	core-shell	silica (C18)	919[e]	0.5	0.9900
13	Phenomenex	100 × 2.1	1.3	88	core-shell	silica (C18)	925[e]	0.5	0.9939
14	Phenomenex	100 × 2.1	1.3	88	core-shell	silica (C18)	945[e]	0.5	0.9867
15	Agilent MiniMix-B	250 × 4.6	10	mixed	fully porous	PS-DVB[b]	133[e]	2	0.9730
16	Agilent Mixed-C	100 × 4.6	5	mixed	fully porous	PS-DVB	132[e]	1	0.9996
17	Agilent Mixed-D	300 × 7.5	5	mixed	fully porous	PS-DVB	144[e]	1.34	0.9988
18	Styragel HR5	300 × 7.8	5	unknown	fully porous	PS-DVB	28[e]	1	0.9995
19	Agilent PLGel 10^2	300 × 7.5	5	100	fully porous	PS-DVB	130[e]	3	0.9451
20	Agilent PLGel 10^4	300 × 7.5	5	10000	fully porous	PS-DVB	127[e]	2.5	0.9982
21	Agilent PLGel 10^5	300 × 7.5	5	100000	fully porous	PS-DVB	123[e]	3	0.9983
22	ZORBAX Eclipse+ RRHD	150 × 2.1	1.8	95	fully porous	silica (C18)	957[e]	0.9	0.9983

[a] Length × internal diameter.
[b] Polystyrene-divinylbenzene.
[c] Correlation coefficient of the calibration curve fit to the polystyrene standard elution time data points.
[d] Limited by maximum desirable flow rate.
[e] Limited by maximum desirable back pressure.

wavelength was 254 nm. We found it necessary to employ a sampling rate of 80 Hz, as lower sampling rates affected the observed peak shape and width of the unretained signal. The flow rates used on each column are specified in Table 1. The injection volume was 1 μL. For measuring van Deemter curves, a sample of Sudan IV was injected at 0.2, 0.4, 0.6, 0.8, 1.0, 1.5 and 2.0 mL min^{-1}. The mobile phase was acetonitrile. The detection wavelength was 500 nm at a sampling rate of 80 Hz.

3. Results & discussion

To gain insight in the separation properties of core-shell particle columns, calibration curves were recorded using a range of polystyrene (PS) standards for all columns. Fig. 1 displays the calibration curves obtained for column 4 (core-shell particles, 150 mm length × 4.6 mm i.d., 2.6 μm particle diameter) at flow rates of 0.2 (red curves; ♦), 0.5 (green curves; ■), 1.0 (orange curves; ▲) and 4.0 (blue curves; ●) mL min^{-1}. These calibration curves were constructed by plotting the nominal average relative molar mass (M_r; dimensionless, setting a mass of 12 for the ^{12}C isotope) against the dimensionless time τ (defined as t_e/t_0). By using τ, the effects of the compressibility of THF (*ca.* 1% per 10 MPa) and eventual variations in the pump's accuracy at different flow rates and pressures are accounted for [8] (see Supplementary Material Figs. S4 and S5 for calibration curves plotted against the apparent elution volume, *i.e.* the set flow rate multiplied by the elution time). The curves largely follow the expected behaviour in SEC, but several interesting observations can be made. First of all, the curves suggest the presence of a strong slalom-chromatography [13] effect. Slalom-chromatography is a flow dependent, hydrodynamic phenomenon, where the coils of longer molecules are elongated as they migrate through the column as a result of the sheering forces arising from the laminar flow. The effect of flow rate on these long molecules can

Table 2
The specified molar masses and dispersities of the polystyrene standards used in this study.

M (g mol^{-1})	log M	Dispersity
580	2.763	1.11
980	2.991	1.1
1990	3.299	1.05
9920	3.997	1.05
13,880	4.142	1.02
19,880	4.298	1.02
52,400	4.719	1.02
70,950	4.851	1.03
299,400	5.476	1.02
735,500	5.867	1.02
1,373,000	6.138	1.04
2,061,000	6.314	1.05
2,536,000	6.404	1.03
3,053,000	6.485	1.03
3,742,000	6.573	1.04
7,450,000	6.872	1.07
13,200,000	7.121	1.13

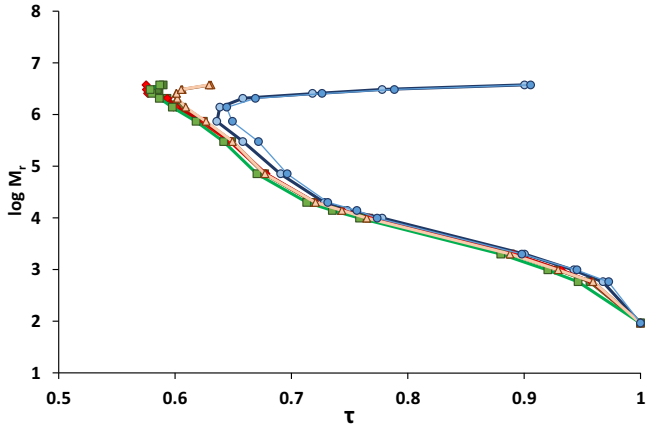

Fig 1. Overlay of calibration curves obtained for column 4 (core-shell, 150 × 4.6 mm, 2.6 μm) at a flow rate of 0.2 (red curves; ♦), 0.5 (green curves; ■), 1.0 (orange curves; ▲) and 4.0 (blue curves; ●) mL·min^{-1}.(For interpretation of the references to colour in this figure legend, the reader is referred to the web version of this article.)

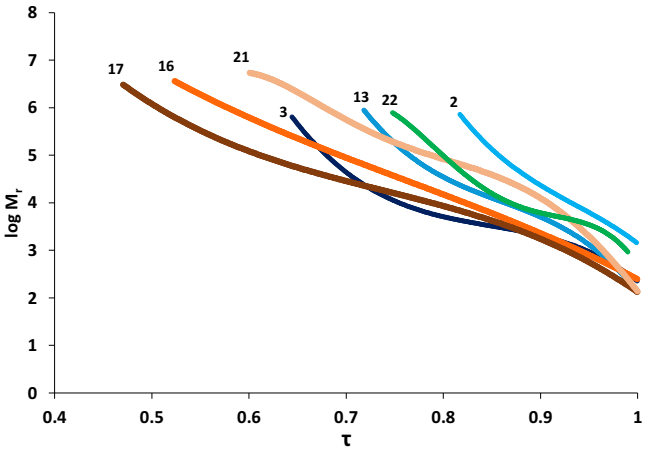

Fig. 2. Overlay of fitted calibration curves for a selection of investigated columns (see Supplementary Data Fig. S6 for an overview of modelled calibration curves of all investigated columns).

be characterized using the ratio of hydrodynamic forces to Brownian forces. This ratio is known as the Deborah number and is defined as [14]

$$De = k_{PB}\left(\frac{\tilde{v}}{d_p}\right)\frac{6.12\Phi\eta r_G^3}{RT} \quad (6)$$

where k_{PB} is a constant which describes the elongation rate within a porous media channel depending on the structure of the packed bed (k_{PB} = 6.3 [15]), $\tilde{v}$ the superficial flow velocity (m·s^{-1}), Φ the Flory-Fox parameter ($\Phi = 2.5\cdot10^{23}$ mol^{-1} [16]), η the viscosity of THF (η = 0.46 mPa·s), r_G the radius of gyration of the PS polymer molecule in μm ($r_G = 1.39\cdot10^{-5}\,M_r^{0.588}$), R the gas constant and T the absolute temperature (T = 298.15 K). At 4.0 mL min^{-1} the Deborah numbers for the polymers with specified molar masses of 2,536,000 and 3,742,000, were 1.1 and 2.1, respectively. With Deborah numbers larger than 0.1 indicating possible polymer deformation, these high Deborah numbers support slalom chromatography as a plausible explanation for the observed behaviour of very-high-molar-mass standards [14,15,17,18].

As expected [13], the slalom effect is more apparent at higher flow rates. For example, at 0.5 mL·min^{-1} (green curves; ■), the slalom-effect is only apparent for polystyrene standards with $M_r \geq 3\cdot10^6$, whereas at 4.0 mL·min^{-1} (blue curves; ●) this is already the case for PS standards with $M_r \geq 1.4\cdot10^6$. More interestingly, however, is an ostensive shift in the exclusion limit. For molar masses approaching 10^6 and upward the observed curve results from a combination of size-exclusion, hydrodynamic-chromatography (HDC) and slalom effects, the relative magnitudes of which are affected by the flow rate. The lowest value of τ observed does, therefore, not correspond to a simple "exclusion limit".

To obtain the best resolution in the shortest possible time, we chose to focus on the data recorded at the highest possible flow rate (up to a maximum of 4 mL/min, because of instrument considerations) within the maximum allowed pressure specified for the column (with a safety margin to allow for possible pressure spikes, *e.g.* upon injection). Calibration curves were recorded for each investigated column. The flow rates used and backpressures observed are listed in Table 1. A third or fifth-order polynomial (whichever best described the data [19]) was fitted through the relevant section of the calibration curve (*i.e.* excluding the slalom section). A selection of fitted calibration curves is displayed in Fig. 2 (see Supplementary Data Fig. S6 for an overlay of all recorded calibration curves).

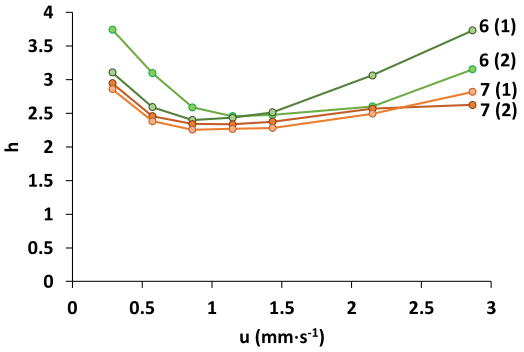

Fig. 3. Examples of duplicate van Deemter curves obtained for columns 6 and 7 which feature core-shell stationary phase packings. Mobile phase: acetonitrile; analyte: Sudan IV; detection at 500 nm.

A clear distinction can be made between the calibration curves of fully porous (curves 16, 17, 21) and core-shell particles (curves 2, 3 and 13). The calibration curves of the columns with fully porous particles appear more flat and extend across a broader molar mass range. These observations are logical consequences of the mixed-bed stationary phases of columns 16, 17 and 21. The curves of the core-shell columns 2, 3 and 13 extend over a narrower V_e-range which is related to their reduced pore volume. Interestingly, the curve of column 22 (fully porous, 1.8 μm particles) also occupies a narrow domain in elution volume, which would suggest a pore volume similar to those of the core-shell columns, despite the absence of a solid-core in the stationary phase particles.

The key objective of this study was to compare packing materials (*i.e.* core-shell *vs.* fully porous), rather than specific columns. Very efficient columns are attractive, but their performance may easily be affected by extra-column band broadening effects. To concentrate on the key issues of the present study, we opted to use an average column efficiency to estimate the separation potential of each material. A reduced plate height of h = 3 was used in all cases. It is feasible to obtain estimates of the true column band broadening (corrected for extra-column effects and the polydispersity of polymeric standards). However, such measurements are quite involved [8,20] and a number of different columns would need to be tested to establish information pertaining to the packing material, rather than to a specific column. To ensure that a value of h = 3 was representative, van Deemter curves were measured using Sudan IV as a totally permeating analyte in a 100% acetonitrile mobile phase. This dye allowed the clear recording of an undisturbed analyte peak at a wavelength of 500 nm. Fig. 3 displays representative van Deemter curves recorded for two columns packed with core-shell particles. The curves show minimum reduced-plate height values well below h = 3, which are in agreement with efficiency values reported in literature for core-shell stationary phases [11]. A value of h = 3 can be seen as a conservative estimate for core-shell columns. The same reduced plate height value (h = 3) was also used for all columns packed with fully porous particles, which may be optimistic for columns packed with relatively large particles operated at high flow rates.

Fig. 2 indicates a somewhat lower selectivity range for core-shell columns, which is expected because of their smaller pore volumes. However, the essential performance criterion in any separation is resolution rather than selectivity range. Therefore, the normalized specific resolution, or packing resolution factors, (R^*_{sp}) were calculated for each kind of packing material (i.e. according to equation 5 for each molar mass. At each point the first derivative of the calibration curve was used to determine the slope b. The value of σ was obtained from the elution time of the toluene marker and h = 3. The resulting R^*_{sp} *vs.* log M_r curves for a selection of columns are shown in Fig. 4 (see Supplementary Material Fig. S7 for the R_{sp} and R^*_{sp}

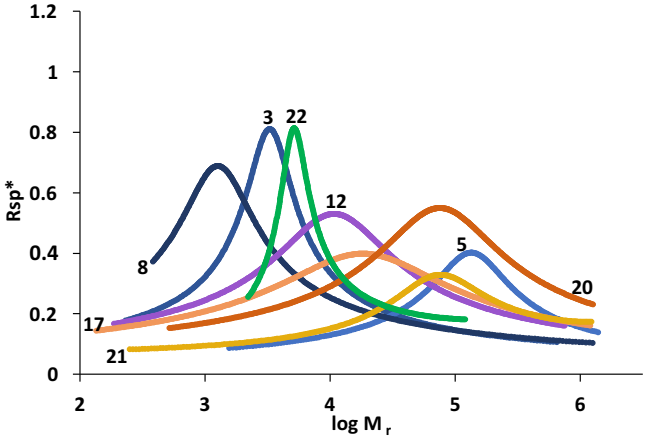

Fig. 4. Overlay of plots of the normalized specific resolution (R_{sp}*) against the relative nominal mass (M_r) for several columns. The number in parentheses indicates the iteration number.

curves for all investigated columns). For several of the core-shell particle columns, the curves (Fig. 4; curves 3 and 8) show high R^*_{sp} values which result from the low slopes of the calibration curves around specific M_r-ranges in combination with the small particle diameters. Fully porous 1.8-μm particles (curve 22) shows a similar kind of R^*_{sp} curve. The core-shell 1.3-μm particles (Fig. 4; curve 12) show a broader, lower curve, because the calibration curve is somewhat steeper, extending across a broader range in log M_r. The shape of the R^*_{sp} curves can be related to the pore-size distribution (PSD) of the particles used. Clearly, the fully porous 1.8-μm particles (curve 22) show the narrowest PSD. The PSD of the core-shell particles (curves 3, 5, 8 and 12) are significantly broader. Some of the investigated core-shell particles were modified with C18 chains. For example, packing material 8 (C18) was obtained by modifying the surface of packing material 3 (silica). It is seen in Fig. 4 that this causes the curve to shift to the left, suggesting that the pores become somewhat narrower as a result of the presence of the C18 layer. The curves representing the conventional fully-porous (curves 17, 20 and 21) underline the relatively broad range of applicability of such columns, especially for the mixed-D column (curve 17), which is packed with a mixture of particles with different PSDs. The resolution that is attainable with such columns is also limited by the relatively large particle size.

It should be noted that the R^*_{sp} curves in Fig. 4 are based on the third or fifth-order polynomial fits of the calibration curve to the recorded PS elution times for each column. While great care was taken to accurately fit the curve, some deviations from the true points will always exist. Essentially, the calibration curves represent a realistic, but smoothed picture of reality. When using all individual data points, the curves become much more erratic and the M_r value at which the highest R^*_{sp} is observed may shift slightly.

Having established that core-shell particles are potentially favourable in terms of (specific) resolution, we now focus our attention on the required analysis time. This is especially critical for the application of SEC as a second-dimension separation in LC × LC. Fig. 5 displays the specific resolution plotted against the elution time for each packing material at three selected relative molar masses; 5000 (Fig. 5A), 20,000 (Fig. 5B) and 100,000 (Fig. 5C). The logarithmic scale of the horizontal axis implies great differences in analysis time for the different points in the scatter plots. The core-shell particles (●) form the fast group (on the left in the figures), together with the smallest fully porous particles (▲; green color). The common LC paradigm that increasing resolution comes at the expense of longer analysis times seems not to hold in the present case. Depending on the molar mass of the polymer

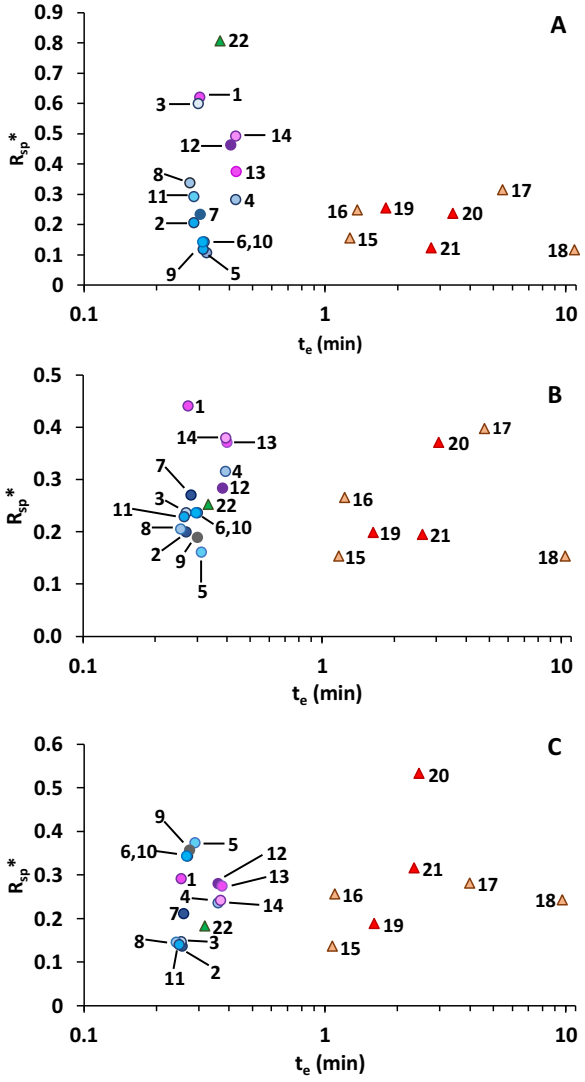

Fig. 5. Scatter plots of the normalized specific resolution (R_{sp}*) against the elution time of a compound with a relative molar mass of A) 5000, B) 20,000 or C) 100,000. Note that the x-axis is plotted on a logarithmic scale. The numbers refer to the specific columns listed in Table 1.(For interpretation of the references to colour in text, the reader is referred to the web version of this article.)

analytes to be studied, similar or better resolution can be obtained much more rapidly with many of the core-shell particles in a much shorter time than with conventional fully-porous materials (▲). Mixed-bed packings with various pore-sizes (▲; orange color) are applicable across a very broad range of analyte M_r. They cannot be expected to give rise to a similar specific resolution as (core-shell or fully porous) particles with specific pore-sizes. Therefore, we also included fully-porous particles with specific pore-sizes in the comparison (▲; red color). Such columns will show high specific resolution values in specific ranges (e.g. column 20 at M_r = 100,000) in analysis times typical for conventional particles. Core-shell particles are shown to be always attractive in terms of analysis time and at least competitive in terms of resolution. If core-shell materials with suitable pore-size distributions are available (e.g. for low-molar-mass polymers with $M_r \approx 5000$, see Fig. 5A) core-shell columns may be attractive in terms of both speed and resolution.

In order to achieve good resolution across a broad molar-mass range, some contemporary SEC columns utilize “mixed-bed” packings featuring a range of pore sizes. Alternatively, different pore sizes may be combined by employing several columns in series. As is shown in Fig. 4, the core-shell stationary phase columns available

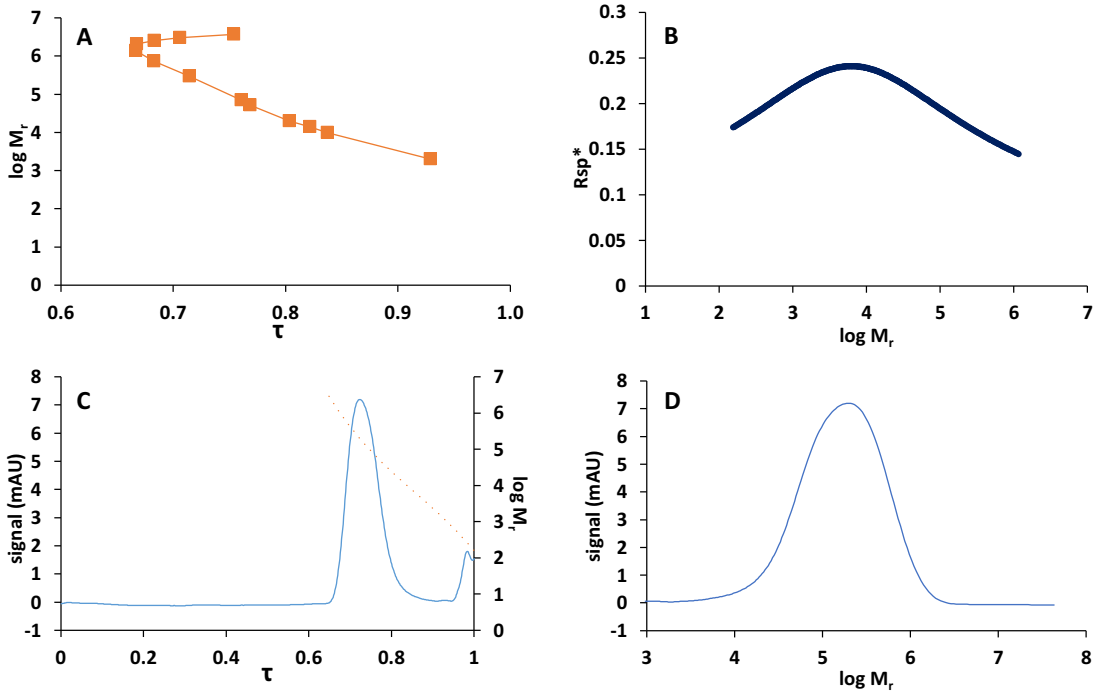

Fig. 6. A) Calibration curve, B) R_{sp}*-plot for columns 3, 8 and 10 coupled in series. C) A SEC chromatogram of a broad polystyrene standard with a specified mass of approx. 200,000 using this combination of columns with the modelled calibration curve (dotted line) as overlay, and D) the molar mass distribution of the broad polystyrene standard. The continuous well-shaped peak in Fig. 6C suggests the absence of pore-size mismatch for the combination of columns.

for this study each featured PSDs that are relatively broad, resulting in a reasonable, yet limited application window. To obtain a very broad application range in a single separation, three columns were coupled: column 10 (328 Å, C18-modified), column 3 (98 Å, silica) and column 8 (98 Å, C18-modified). A calibration curve and an R^*_{sp}-plot were established (Fig. 6). As expected, the coverage of the molar-mass range improved, at the expense of a more modest normalized specific resolution (R^*_{sp}-). The smoother calibration curve shown in Fig. 6A was highly encouraging. Good SEC performance was demonstrated by injecting a broad PS standard, which yielded a single well-shaped peak in the SEC chromatogram (Fig. 6C). The molar mass distribution (Fig. 6D) confirmed the reported molar mass of approximately 200,000. However, by coupling three columns, the maximum flow rate (2 mL/min, 782 bar; down from 4 mL/min) was significantly reduced. The longer length of the combined columns and the lower maximum flow rate together result in a six-fold increase in the analysis time. To achieve high-resolution, fast separations across a broader M_r range the most-attractive option is to prepare mixed-bed columns containing core-shell particles with different pore size distributions. A somewhat lower resolution cannot be avoided (see Fig. 6B), but the high speeds shown in Fig. 5 can be maintained.

One difference between the investigated "conventional" and core-shell stationary phase columns that has not yet been mentioned is that most conventional columns comprised polystyrene-divinylbenzene (PS-DVB) polymeric particles, whereas the core-shell columns contained silica particles. While excellent control over the pore-size distribution of PS-DVB particles has been achieved, their potential for yielding high chromatographic efficiencies is inferior to that of rigid silica particles. The latter can withstand much higher operational and packing pressures. To cover this angle we included a column packed with fully-porous silica particles (column 22, see Table 1). It is clear that such a column may also yield a high specific resolution in a relatively short time for analyte polymers of suitable size (in the case of column 22 around 5000, see Fig. 6A). However, the correct application of columns packed with sub-2-μm particles requires instrumentation capable of operating at very high-pressures and rigorous control of extra-column band-broadening effects. Further investigations are required for a complete comparison of core-shell and fully porous silica packing materials for SEC. Finally, in this study, the investigated conventional columns largely featured relatively large particle diameters in comparison with the core-shell particles. The C-term contribution to the column band broadening is expected to result in $h \gg 3$ at the investigated maximum flow rates. Thus, the present study provides a conservative assessment of the advantages of using core-shell and sub-2-μm particles in size-exclusion chromatography. We are currently investigating ways to take the various contributions to band broadening in SEC into account in a more rigorous manner.

5. Conclusion

We have demonstrated the feasibility of using core-shell materials in size-exclusion chromatography to obtain high SEC resolution within very short analysis times. The reduced pore volume relative to fully porous particles is compensated for by an increase in efficiency. While the conventional columns specifically developed for SEC perform more evenly across a broader range of analyte molar masses, the investigated core-shell columns exhibited excellent performance across more limited ranges, depending on the pore size. It seems entirely feasible that fast, efficient and broadly applicable SEC columns can be developed using core-shell technology. Analysis times of 0.4 min or less were observed, which is very promising for application as a second-dimension separation in an LC × LC separation system.

Acknowledgement

The MANIAC project is funded by the Netherlands Organisation for Scientific Research (NWO) in the framework of the Programmatic Technology Area PTA-COAST3 of the Fund New Chemical

Innovations (project C.2322.0291). Phenomenex is acknowledged for supporting this work. Noor Abdulhussain and Sanne Berbers are acknowledged for their assistance.

Appendix A. Supplementary data

Supplementary data associated with this article can be found, in the online version, at http://dx.doi.org/10.1016/j.chroma.2016.12.015.

References

[1] A.M. Striegel, W.W. Yau, J.J. Kirkland, D.D. Bly, Modern Size-Exclusion Liquid Chromatography, second ed., John Wiley & Sons, Inc., Hoboken, NJ, USA, 2009, http://dx.doi.org/10.1002/9780470442876.
[2] M.A.R. Meier, U.S. Schubert, Combinatorial polymer research and high-throughput experimentation: powerful tools for the discovery and evaluation of new materials, J. Mater. Chem. (2004) 3289–3299.
[3] A. van der Horst, P.J. Schoenmakers, Comprehensive two-dimensional liquid chromatography of polymers, J. Chromatogr. A. 1000 (2003) 693–709, http://dx.doi.org/10.1016/S0021-9673(03)00495-3.
[4] E. Uliyanchenko, P.J.C.H. Cools, S. van der Wal, P.J. Schoenmakers, Comprehensive two-dimensional ultrahigh-pressure liquid chromatography for separations of polymers, Anal. Chem. 84 (2012) 7802–7809, http://dx.doi.org/10.1021/ac3011582.
[5] D.R. Stoll, X. Li, X. Wang, P.W. Carr, S.E.G. Porter, S.C. Rutan, Fast, comprehensive two-dimensional liquid chromatography, J. Chromatogr. A 1168 (2007) 3–43, http://dx.doi.org/10.1016/j.chroma.2007.08.054.
[6] P. Dugo, F. Cacciola, T. Kumm, G. Dugo, L. Mondello, Comprehensive multidimensional liquid chromatography: theory and applications, J. Chromatogr. A 1184 (2008) 353–368, http://dx.doi.org/10.1016/j.chroma.2007.06.074.
[7] S.T. Popovici, P.J. Schoenmakers, Fast size-exclusion chromatography?theoretical and practical considerations, J. Chromatogr. A 1099 (2005) 92–102, http://dx.doi.org/10.1016/j.chroma.2005.08.071.
[8] E. Uliyanchenko, P.J. Schoenmakers, S. Van Der Wal, Fast and efficient size-based separations of polymers using ultra-high-pressure liquid chromatography, J. Chromatogr. A 1218 (2011) 1509–1518, http://dx.doi.org/10.1016/j.chroma.2011.01.053.
[9] M. Janco, E.S.P. Alexander IV, D. Morrison, Ultra-high performance size-exclusion chromatography of synthetic polymers: demonstration of capability, J. Sep. Sci 36 (2013) 2718–2727, http://dx.doi.org/10.1002/jssc.201300444.
[10] W.W. Yau, J.J. Kirkland, D.D. Bly, H.J. Stoklosa, Effect of column performance on the accuracy of molecular weights obtained from size exclusion chromatography (gel permeation chromatography), J. Chromatogr. A 125 (1976) 219–230, http://dx.doi.org/10.1016/S0021-9673(00)93821-4.
[11] F. Gritti, I. Leonardis, J. Abia, G. Guiochon, Physical properties and structure of fine core-shell particles used as packing materials for chromatography. Relationships between particle characteristics and column performance, J. Chromatogr. A 1217 (2010) 3819–3843, http://dx.doi.org/10.1016/j.chroma.2010.04.026.
[12] Y. Vanderheyden, D. Cabooter, G. Desmet, K. Broeckhoven, Isocratic and gradient impedance plot analysis and comparison of some recently introduced large size core-shell and fully porous particles, J. Chromatogr. A 1312 (2013) 80–86, http://dx.doi.org/10.1016/j.chroma.2013.09.009.
[13] J. Hirabayashi, N. Ito, K. Noguchi, K. Kasai, Slalom chromatography: size-dependent separation of DNA molecules by a hydrodynamic phenomenon, Biochemistry 29 (1990) 9515–9521, http://dx.doi.org/10.1021/bi00493a004.
[14] D.A. Hoagland, R.K. Prud'homme, Hydrodynamic chromatography as a probe of polymer dynamics during flow through porous media, Macromolecules 22 (1989) 775–781, http://dx.doi.org/10.1021/ma00192a044.
[15] R. Haas, F. Durst, Viscoelastic flow of dilute polymer solutions in regularly packed beds, Rheol. Acta. 21 (1982) 566–571, http://dx.doi.org/10.1007/BF01534349.
[16] V.G.V. Schulz, H. Baumann, Thermodynamisches verhalten, expansionskoeffizient und viskositätszahl von polystyrol in tetrahydrofuran, Die Makromol. Chemie 114 (1968) 122–138, http://dx.doi.org/10.1002/macp.1968.021140109.
[17] E. Venema, J.C. Kraak, H. Poppe, R. Tijssen, Packed-column hydrodynamic chromatography using 1-μm nonporous silica particles, J. Chromatogr. A. 740 (1996) 159–167, http://dx.doi.org/10.1016/0021-9673(96)00135-5.
[18] E. Uliyanchenko, S. van der Wal, P.J. Schoenmakers, Deformation and degradation of polymers in ultra-high-pressure liquid chromatography, J. Chromatogr. A 1218 (2011) 6930–6942, http://dx.doi.org/10.1016/j.chroma.2011.08.014.
[19] Y. Vander Heyden, S.T. Popovici, P.J. Schoenmakers, Evaluation of size-exclusion chromatography and size-exclusion electrochromatography calibration curves, J. Chromatogr. A 957 (2002) 127–137.
[20] F. Gritti, G. Guiochon, Application of the general height equivalent to a theoretical plate equation to size exclusion chromatography. study of the mass transfer of high-Molecular-Mass compounds in liquid chromatography, Anal. Chem. 79 (2007) 3188–3198, http://dx.doi.org/10.1021/ac0623742.